Chronologie éruptive de l’arc récent dans le compartiment nord de la Martinique

The eruptive history of Plio-Pleistocene volcanism in northern Martinique Island (French West Indies): new K-Ar ages and volume calculations.

Germa Aurélie * [1]; Quidelleur Xavier[1]; Labanieh Shasa[2]; Lahitte Pierre[1] ; Chauvel Catherine[2].

[1]*: Laboratoire de Géochronologie Multi-Ttechniques - UMR CNRS-UPS11 8148 IDES, Département des Sciences de la Terre, Bat. 504, Sciences de la Terre, Université Paris Sud 11, 91405 Orsay Cedex, FRANCE*

[2]*: LGCA, Universite J. Fourier, Maison des Geosciences, 1381, rue de la Piscine, 38400 St-Martin d'Heres FRANCE*

---

* Corresponding author: Germa Aurélie

Phone : + 33 (0) 1 69 15 67 71

e-mail: aurelie.germa@u-psud.fr

Word count:

- abstract: 353
- text: 6527

To be submitted to: Journal of Volcanology and Geothermal Research

Abstract

Martinique (14°N, 61°W) is the Lesser Antilles Island where the most complete volcanic history of the arc can be found. However, most studies have been restricted to Mount Pelée volcano, more particularly to the destructive 1902 and 1929 A.D. eruptions, rather than on the older zones from the recent arc (Morne Jacob, Pitons du Carbet and Mount Conil complexes). We have dated thirty-one representative samples from the northern volcanic complexes by K-Ar, based on the Cassignol-Gillot technique. Together with these radiometric ages, morphological constraints and field observations have helped us to better reconstruct the volcanic history of the Morne Jacob, Pitons du Carbet and Mount Conil complexes, and to characterize their relationship with the active volcano of Mount Pelée.

Our results show that the Morne Jacob, the largest shield volcano of the Lesser Antilles, has a longer history than previously inferred: the different stages of activity range between 5.5 and 1.5 Ma. A large basaltic to andesitic shield volcano was first built between 5.5 and 2.1 Ma. At the end of this stage, creeping probably affected its north-eastern flank. Then, more basic magmas erupted at the central vent and from peripheric fissures down to the Caribbean coast between 2.0 and 1.5 Ma. Piton du Carbet complex is younger than estimated before: a first stage of activity occurred with the construction of an andesitic volcano between 1 Ma and 600 ka, which ended by a large flank collapse southwest directed. It has been suggested that the loss of lithostatic load favoured more basic magma ascent and eruption of Pitons du Carbet s.s. inside the depression at about 334 ± 6 ka. Mount Conil and Mount Pelée constitute the northernmost and youngest compartment of the island. Mount Conil complex started its activity while the Carbet complex was still active, with andesites emitted between 543 ± 8 ka and 189 ± 3 ka, while the recent activity remained within the Mount Pelée. Finally, our combined approach based on geochronological, geochemistry, geomorphological and

fieldwork studies, allow us to propose a general evolution model for the recent arc volcanism in northern Martinique Island, from 5.5 Ma to present.

Keywords: Lesser Antilles, Martinique, K-Ar dating, Plio-Pleistocene volcanism

1. Introduction

The aim of this study is to determine the volcanic evolution of the recent Lesser Antilles Island arc in northern Martinique Island by constraining the building and destructive rates of the different volcanic complexes. Determining the growth rate and the evolution of a volcano is critical to understand periodicity and frequency of volcanic episodes, and to complete the global database of volcanic output rates. Moreover, coupled with petrographic and geochemical studies, geochronological investigations can provide insights into the compositional evolution of a volcanic complex.

Despite the fact that the evolution of the active volcanoes from the Lesser Antilles Island arc are relatively well documented, few reliable data on eruptive rates and chronologies of the whole islands are available (Guadeloupe: Samper et al., 2007; Montserrat: Harford et al., 2002). However, this kind of study has been well developed in recent years, for other arc stratovolcanoes built on oceanic crust (Seguam Island, Jicha et al., 2006) as well as on continental setting (Parinacota, Hora et al., 2007; Ceboruco-San Pedro, Frey et al., 2004; Tequila Volcanic field, Lewis-Kenedi et al., 2005; Mount Baker, Hildreth et al., 2003a; Mount Adams, Hildreth et al., 1994; Katmai cluster, Hildreth et al., 2003b). These studies

have shown that eruptive rates are highly variable, with peak rates during cone building ranging from 0.2 to 5 km^3 / ka for recent volcanism, younger than 1 Ma.

Martinique, located in the central Lesser Antilles arc, is an 1100 km^2 island built during the last 26 Myr. Its northern compartment is made of four Plio-Pleistocene volcanic complexes of lavas with compositions ranging from 48.6 % to 60.6 % SiO_2. Previous K-Ar dating of whole-rock samples indicated a 5.5 Myr history for the whole northern compartment (Westercamp et al., 1989) with a poor precision of about 5 – 7 % and a questionable reliability. Recent geochronological studies on Basse Terre de Guadeloupe (Blanc, 1983; Carlut et al., 2000; Samper et al., 2007), and at Montserrat (Harford et al., 2002) have shown a large discrepancy and inadequacy, both regarding magnetic polarity and geological evolution, within the results published during the eighties (Andreieff et al., 1988; Andreieff et al., 1976; Bellon et al., 1974; Briden et al., 1979; Nagle et al., 1976) due, most probably, to the use of whole-rock dating of weathered samples.

The purposes of this study are to use high-precision $^{40}K/^{40}Ar$ geochronology and geochemical analyses to (1) better constrain the duration of activity of each building stage, (2) quantify the volumetric evolution of each volcanic complex, (3) estimate the eruptive rates, and (4) establish the precise chronologic history of the northern Martinique Island.

2. Geological setting

2.1. Lesser Antilles Island arc

Martinique is located in the central part of the Lesser Antilles Island arc, which results from the westward subduction of the Atlantic plate under the Caribbean plate (Fig. 1a).

Whereas in the southern part of the arc, volcanic activity occurred along a single SW-NE axis, the northern part, which experienced a westward jump of the volcanic front, is divided into two distinct branches (Fig. 1a, Fink, 1972). The inactive arc lies to the east (dashed line in Fig. 1a) where volcanic activity took place from the Eocene to the Oligocene (Bouysse et al., 1979; Westercamp, 1972; Germa et al., 2008). From Grenada to Saba, the islands that constitute the internal arc are called the Volcanic Caribbees (black line, Fig. 1a), where volcanism is currently active since the early Miocene (Bouysse et al., 1979; Westercamp, 1972). Due to its central position where the two northern arcs merge, Martinique is the Lesser Antilles Island where the most complete history of the arc can be found, from 20 Ma to present (Briden et al., 1979; Westercamp et al., 1989).

2.2. Martinique Island

With an area of 1100 km^2, Martinique is the largest island of the arc. It lies at 14°N and 61°W, between Dominica and Saint Lucia islands (Fig. 1a).

Volcanic activity has been almost continuous from the Oligocene to historic times, and eight volcanic units have been identified (Fig1b; (Andreieff et al., 1988; Grunevald, 1965; Westercamp, 1972; Westercamp et al., 1989; Westercamp et al., 1980)): (1) the Basal Complex and Saint Anne series (26 – 20 Ma, Germa et al., 2008), (2) the Vauclin-Pitault submarine chain (17 – 10 Ma), (3) the South western volcanism (8.5 – 6.5 Ma), (4) the Trois Ilets volcanism (3.5 - 0.6 Ma), (5) the Morne Jacob volcano (5.5 – 2.2 Ma), (6) the Carbet complex (2 – 0.9 Ma), (7) the Conil Complex (1.2 – 0.4 Ma) and (8) the Mount Pelée volcano. We describe below these last four Plio-Pleistocene complexes and associated ages previously available for the northern Martinique.

2.2.1. Morne Jacob Volcano

The construction of the Morne Jacob shield Volcano, the largest volcanic edifice of the whole Lesser Antilles Island arc (> 350 km^2), began about 5 Myr ago, with basaltic to andesitic hyaloclastites and subaerial lava flows emitted from ENE-WSW fractures (Westercamp et al., 1989). These authors identified a first building stage that occurred between 5.5 and 4.1 Ma (light blue in Fig. 2) followed by a second phase from 2.7 to 2.2 Ma (dark blue in Fig. 2) with massive lava flows reaching the Caribbean coast.

2.2.2. Carbet complex

The Carbet complex was constructed on the western flank of Morne Jacob volcano (Fig. 2). The building of an andesitic edifice (light brown in Fig. 2) has been estimated between 2 and 1 Ma ago based on the dating of pyroclastic flow deposits and few lava flows. This stage ended with the emplacement of lava domes then dated at about 1 Ma (Westercamp et al., 1989). This younger limit has been recently challenged by Samper et al. (2008) who found an age of 770 ± 11 ka (Table 1) for Piton Gelé, which is located at the northeastern limit of the complex, whereas an older age of 1.06 ± 0.10 Ma was previously inferred (Westercamp et al., 1989). A flank-collapse of about 30 – 40 km^3 (Boudon et al., 2007) occurred between 1.86 ± 0.03 Ma and 341 ± 5 ka (Samper et al., 2008), yielding a horseshoe-shaped structure opened to the west (white line, Fig. 2) and characterized by massive debris-avalanche deposits outcropping along the Caribbean coast, while, surprisingly, no associated such deposits have been recognized offshore (Boudon et al., 2007). The Pitons du Carbet s.s. are a group of seven voluminous lava domes, plus 5 isolated smaller ones, of andesitic composition, emplaced inside the horseshoe structure (dark brown, Fig. 2). Five of them are

higher than 1 000 m: Piton Lacroix (1 196 m), Piton Boucher (1 070 m), Piton de l'Alma (1 105 m), Piton Dumauzé (1 109 m), and Morne Piquet (1 160 m). A mean emplacement age of 337 ± 5 ka (Table 1) has been obtained for three of these lava domes (Alma, Morne Piquet and Piton Man Roy; Samper et al., 2008).

2.2.3. Conil complex and Mount Pelée

Between 1 and 0.4 Ma, the Mount Conil complex (blue crosshatch, Fig. 2) was built in the northern end of the island. It is composed of andesitic breccias, lava domes and lava flows. The end of its activity corresponds to the beginning of the building of Mount Pelée Volcano (pink in Fig. 2, Westercamp et al., 1989). Because only sparse geochronological data are available for Mount Conil (Table 1), timing of its activity is not well known but seems to have occurred between: 1.20 ± 0.20 Ma (Andreieff et al., 1988) and 0.4 ± 0.2 Ma (Bellon et al., 1974). Three eruptive periods have been identified for the recent Mount Pelée within two main stages called the Paléo and Néo-Pelée. These stages consist of successions of construction and destruction periods (Le Friant et al., 2003). This volcano experienced three major flank collapse events (D1, D2, D3), respectively at 100, 25 and 9 ka (black lines, Fig. 2a), followed by the building of a new cone inside each horseshoe-shaped structure (Le Friant et al., 2003). Some U – Th ages (Table 1) have been obtained on lava domes that were affected by the flank collapse events, permitting the chronological reconstruction of the Mount Pelée history, and more than a hundred of ^{14}C ages available allow a satisfactory understanding of the last 40 kyr of activity (Boudon et al., 2005). Twenty-eight magmatic eruptions occurred during the last 16 kyr, with ten plinian and eighteen dome-forming eruptions, plus an unknown number of phreatomagmatic and phreatic eruptions (Boudon et al., 2005). Since the European settlement, two phreatic eruptions occurred in 1792 and 1851,

and two magmatic dome-forming eruptions in 1902 - 1904 and 1929 - 1932. The flanks of Mount Pelée are mainly composed of pyroclastic flow deposits related to three types of activity (St Vincent, Plinian and Pelean; Boudon et al., 2005). Ninety percent of its subaerial deposits are volcaniclastics, and minor lava domes and flows are only present near the summit (Aileron lava dome, Morne Macouba, and historic lava domes).

3. Materials and methods

3.1. Sampling technique

During March 2006 and April 2007, 55 fresh lava flows and domes were sampled in Northern Martinique within the Morne Jacob volcano (n = 33, circles in Fig. 2b), Carbet complex (n = 7, diamonds in Fig. 2b), Mount Conil complex (n = 10, squares in Fig. 2b) and Mount Pelée volcano (n = 5, squares in Fig. 2b). At each location, hand-size blocks were sampled for geochronological and geochemical studies. To constrain through time the evolution of each complex, we have chosen the most significant sites and located escarpments, quarries, road cuts, coastal cliffs and rivers after examination of DEM, topographic and geological maps. Indeed, due to the tropical climate, erosion and presence of dense vegetation, outcrops were limited to these specific locations. In a companion paper (Labanieh et al., 2008), major, trace elements and isotopic compositions, obtained on the same samples than those dated here, are presented in details.

3.2. K-Ar Geochronology

Thirty-one samples were carefully selected for K-Ar dating using the Cassignol-Gillot technique on the basis of sample freshness, as confirmed by examination of petrographic thin sections: six for Mount Conil, seven for Carbet complex, and twenty-two for Morne Jacob. K-Ar dating method was chosen because it allows accurate dating of both ancient and young lavas, even with low radiogenic content (Cassignol and Gillot, 1982 ; Gillot and Cornette, 1986).

In order to remove any possible gain of argon (excess argon) coming from fluids circulations or from xenoliths of older basement rocks, and any possible loss of potassium due to weathering, a careful mineralogical separation was performed. Based on phenocrysts size, jaw crushing and sieving at typically 125-250 μm was performed. Grains were ultrasonically washed with deionized water and a 10% nitric acid solution. Heavy liquids were used to keep groundmass in narrow density ranges, typically 2.80 – 2.85 g/cm^3 for basalts, 2.70 – 2.75 g/cm^3 for basaltic-andesites, and to 2.60 – 2.65 g/cm^3 for andesites and dacites. Finally, we have separated groundmass and residual minerals with a Frantz magnetic separator. In some cases (samples 06MT32, 06MT14, 07MT121 and 06MT36), when plagioclases were considered suitable after thin sections examination, they were extracted at density around 2.70 g/cm^3, in order to further support the age obtained on the groundmass.

We measured potassium and argon at the Laboratoire de Géochronologie Multi-Techniques (Orsay, France), from different aliquots of the same mineral preparation, K by flame emission spectroscopy and Ar by mass spectrometry using an instrument similar to the one described in Gillot and Cornette (1986). The relative uncertainty on K measurement is about 1% over a range of K contents between 0.1 and 15%. The limit of detectability of the radiogenic Ar content is presently of 0.1% (Quidelleur et al., 2001) and makes the Cassignol-

Gillot technique especially suitable for very young dating as it allows to obtain K-Ar ages as young as 2 ka with only a few centuries uncertainty (Gillot et al., 2006). Such performance can be achieved because of the very stable analytic conditions of our mass spectrometer, which allows a very accurate atmospheric correction by direct comparison of the dated sample with an air aliquot measured in the exact same Ar pressure conditions. The calibration of the system is obtained by systematic measurements of an air pipette, which is routinely compared to the GL-O standard with its recommended value of 6.679 x 10^{13} at.g^{-1} of radiogenic ^{40}Ar (^{40}Ar *) (Odin, 1982). Such calibration introduces an additional relative uncertainty of 1%, which leads to a total relative age uncertainty of about 1.5% for samples of about 1 Ma. However, for younger samples, the uncertainty due to the atmospheric correction dominates and can amount to 100% for sub-historic samples (with ^{40}Ar* of 0.1 %). Potassium and argon were analyzed at least twice in order to obtain a reproducible age within the range of error determined from periodic replicated measurements of dating standards, such as ISH-G, MDO-G (Gillot et al., 1992) and GL-O (Odin, 1982). For age calculations, decay constant and K isotopic ratios of (Steiger et al., 1977) have been used. A chronological summary of the 31 dated samples is presented in Table 2. All uncertainties quoted here are given at the 1-sigma level. The ages of each sample are also displayed in Fig. 3. As each age has been obtained on distinct lava flows and domes well distributed geographically, they are presented in an age probability spectra (ideogram, Fig. 4), following the formula proposed by Deino and Potts (Deino et al., 1992), to identify periods of construction and/or dormancy.

3.3. Volume estimations

Volume estimates were determined from analysis of the geological map (1:100 000; Westercamp et al., 1989) and the digital elevation model (DEM; 1:50 000) using the

geographical information system (GIS) software ArcGIS 9.1. The DEM is at a scale of 1:50 000 and uses a Universal Transverse Mercator (UTM) projection and the World Geodetic System 84 (WGS 1984) model. In order to evaluate the volumes of volcanic products and edifices, a paleo-topography for each volcanic stage was created using GIS calculations (e.g., local polynomial interpolation), from the present topography of representative structural surfaces, units outlines or watershed crests. Successive three-dimensional surface created represent the basal surface for the next construction stage. As the northern compartment is active since 5.5 Ma at tropical latitudes where erosion is intense, the estimates should be regarded as minimum volumes. Moreover, as we use ages from aerial lava flows, we thus only consider the volumes above sea level. The main imprecision for Martinique Island volume estimates, is that the preserved subaerial deposits represent only a fraction of the total erupted volume because a significant percentage is located below the sea level, has been intruded into the crust, or deposited under the sea during explosive eruptions.

4. Results

4.1. Macro- and microscopic identification

Lavas from Morne Jacob volcano are black basaltic-andesites to dacites. In thin sections, samples from the two eruptive stages are strictly different. The first stage is characterized by porphyritic basaltic-andesites with 5 to 15 % vol. of crystals. The main mineral phase is plagioclase, with sizes ranging from about 200 μm to more than 2 mm. The other minerals are rare crystals of augite and olivine (< 1mm). The microcrystalline

groundmass is made of microliths of plagioclase and clinopyroxene with size range of 40 - 80 μm. The second stage is characterized by porphyric andesites with 20 to 40 % vol. of crystals. The main mineral phase is plagioclase (100 μm - 1 mm), associated with two pyroxenes (hyperstene and augite) with sizes ranging from 100 to 500 μm. The groundmass is fine grained, with plagioclase, pyroxene and glass.

Samples from Carbet complex are grey porphyritic andesites. The most abundant mineral is plagioclase, with sizes of several millimetres, but we observe few amphibole, quartz and biotite with sizes reaching 1 cm. In thin sections, rocks have 25 – 30 % vol. of crystals with sizes ranging between hundreds of □m to 10 mm. The main mineral is plagioclase, associated with clinopyroxene (augite), orthopyroxene (hyperstene), amphibole (hornblende) and quartz. The second stage is characterized by the occurrence of centimetric crystals of biotite and a larger amount of quartz. The groundmass is microcrystalline, with plagioclase, pyroxene and glass.

Lavas sampled within the Conil complex are dark to light grey andesites, with uneven fractures (from clean to granular). Rocks are porphyritic with mineral sizes never exceeding 5 mm. In thin sections, the rock contains 10 to 25 % vol. of crystals; with sizes from hundreds of μm to several mm. Plagioclase is the main mineral, associated with amphibole (hornblende) and hyperstene. Few amounts of augite are associated to amphibole (several μm), whereas it is absent in other cases, where the hornblende exceeds 1 mm in size.

4.2. Morne Jacob Volcano

4.2.1. K-Ar ages

Ages range from 1.53 Ma to 5.14 Ma (Fig. 3, Table 2), with K content between 0.12 and 2.01%, and radiogenic argon content (^{40}Ar*) between 1.4 and 80.5 %. Older basal lava flows, sampled at coastal locations and in deep valleys, have ages from 5.14 ± 0.07 Ma (06MT32) to 4.10 ± 0.06Ma (06MT34). Six samples located in the central area of the complex (06MT25, 06MT30, 06MT10, 06MT13, 06MT20 and 06MT08) have ages between 3.01 ± 0.19 Ma (06MT30) and 2.11 ± 0.03 Ma (06MT10). A sample from the main escarpment above Rivière du Carbet, (06MT19) yields an age of 1.75 ± 0.02 Ma, and another lava flow at the edge of this cliff has a K-Ar age of 1.62 ± 0.02 Ma (06MT16). To the south of the complex, three samples (07MT118, 06MT38 and 07MT101) from the longest lava flows have quite similar ages from 1.93 ± 0.03 Ma to 1.81 ± 0.03 Ma. Finally, Morne Jacob summit itself is dated at 1.53 ± 0.02 Ma (06MT14), and samples from the surrounding crests have ages of 2.04 ± 0.03 Ma (06MT15) and 1.72 ± 0.02 Ma (06MT24) respectively.

4.2.2. Volumes estimates and eruptive rates

Morne Jacob Volcano has a complex geometry. Indeed, it is deeply dissected so that only a minimum surface has been preserved along watershed crests. To model the paleo-topography of the first stage (5.5 to 4.5 Ma), we extracted from the DEM the points located at the boundary between stage 1 and stage 2, as well as the points along watershed crests representative of the minimal surface of lava flows. We thus calculated the best surface fitting

all these points using a local polynomial interpolation. The volume of the shield is then estimated by multiplying the area (493 km^2) by the mean elevation above sea level (204 m), so that we propose a minimum volume of 100 km^3 for the first stage of Morne Jacob. This first shield has been emplaced between 5.5 and 4 Ma, thus we suggest an eruptive rate of 0.066 km^3/kyr. To reconstruct the second shield, without discriminating the two last stages, we used the points of the watershed crests for a local polynomial interpolation, as well as the points located at the boundary between the second stage and the younger volcanic units. We estimate a volume of 110 km^3 above sea level, but only 14 km^3 above the first shield, which yield an eruptive rate of 0.007 km^3/kyr.

4.3. Carbet complex

4.3.1. K-Ar ages

Ages range from 998 ± 14 ka to 322 ± 6 ka (Fig. 3 and Table 2), with K content between 0.76 and 2.01% and $^{40}Ar^*$ between 8.6 and 60.2 %. Two lava domes located at the periphery of the complex, and belonging to the older stage, has been dated at 998 ± 14 ka (Morne Césaire, 06MT36), 893 ± 13 ka (Morne Fumé, 06MT21) and 603 ± 11 ka (Morne Saint Gilles, 07MT123). A lava dome and a lava flow from the Pitons du Carbet s.s. yield the ages of 322 ± 6 and 332 ± 7 ka (06MT37 and 07MT121, respectively, Table 1).

4.3.2. Volume estimates and eruptive rates

We propose a volume of about 50 km^3 above sea level for the first Carbet edifice, which corresponds to only 5 km^3 above the Morne Jacob shield volcano. This edifice has been built between 1 Ma and 600 ka, with a time-average eruptive rate of 0.012 km^3/kyr.

The main difficulty to retrieve the volume of the Pitons du Carbet s.s. is to choose a basal surface. Indeed, we can consider both the outcropping volume only, as well as the deep-seated volume. As we do not have any evidence for a deep contact, we have calculated a maximum volume above sea level of 10 km^3, and a minimum outcropping volume of only 2 km^3 above the reconstructed surface fitting the base of the Piton du Carbet s.s.. These volumes account for eruptive rates between 0.1 and 0.5 km^3/kyr.

4.4. Conil complex

4.4.1. K-Ar ages

Ages range from 543 ± 8 ka to 189 ± 3 ka (Fig. 3 and Table 2), with K content from 0.79 % to 1.49 % and $^{40}Ar^*$ between 0.8 and 27.9 %. Sample 06MT28 taken from a cliff at Grand' Rivière yields an age of 543 ± 8 ka. Sample from Petit Morne (06MT42), to the north-east, has been dated at 384 ± 6 ka, and those from Morne du Céron (06MT18), to the south-west of the complex, at 346 ± 42 ka. Two close lava flows from Morne à Lianes and Ravin de l'eau (06MT48 and 06MT47) have the same age of 207 ± 3 ka. Finally, a prismatic lava flow sampled in Rivière Trois-Bras, at the centre of the complex, yields an age of 189 ± 3 ka (06MT40).

4.4.2. Volumes estimates and eruptive rates

With Mount Pelée which partly covers it, Mount Conil is the youngest volcano of the studied area, and has simply been considered here as a cone for reconstructions. We used the watershed crests that could be representative of the original slopes and extrapolated their profiles. Afterwards, the elevation has been plotted versus the distance of the profile exported, and smoothed using a Bézier curve. We finally apply revolution symmetry of this profile along thirty-two concentric profiles, and iterated the values into a matrix. The grid thus obtained is exported into the ARC GIS workspace to generate a surface using a local polynomial interpolation. We have obtained a cone, slightly concave, with a diameter of 13.5 km, and a maximum elevation of 1167 m. For the considered area A above sea level, we know the mean elevation E_m of all pixels, and we thus estimated the volume V of this cone at 42 km^3, using the following formula: $V = A \times E_m$. Our ages distribution, together with the geological map, indicate that the group of lava domes formed by Morne Sibérie, Piton Mont Conil, Pain de Sucre, Piton Pierreux and Morne Sainte Croix, as well as associated lava flows, erupted later from an east-west fissure on the northern flank of the cone. We also reconstructed the approximate DEM of this group and calculated a volume of 1.3 km^3. We thus estimate the volume of Mount Conil at about 44 km^3 at the time of its building, before any erosion processes or flank collapse event. The time-average eruptive rate of Mount Conil is thus of 0.200 km^3/kyr.

5. Discussions

Our ages display much lower uncertainties (less than 1.5%) than those of about 5 – 7 % obtained by Westercamp et al. (1989, Table 1), which were. This can be explained by the fact that their ages have been obtained with K-Ar dating mostly on whole rock material, which yield higher atmospheric contamination. Moreover, whole rock analyses can also yield too old ages due to argon heritage from older mineral phases (Harford et al., 2002; Samper et al., 2008) or because of undetected K loss due to weathering. On the contrary, our technique reliability is based on a careful separation of mineral phases and preferential analysis of the groundmass phase, which crystallizes last and under atmospheric conditions. It has been shown that the Cassignol-Gillot technique is specially suitable to date Lesser Antuilles lava flows and domes (Blanc, 1983; Carlut et al., 2000; Samper et al., 2007; 2008).

5.1. Morne Jacob

5.1.1. Spatio-temporal evolution

We deduced from the age probability spectra (Fig. 4), which incorporates variable analytical uncertainties (Deino et al., 1992), that the activity to construct Morne Jacob volcano has been almost continuous during 4 Myr, from 5.3 to 1.4 Ma, over a time interval of 3.9 Myr. Within this period, we have identified two main phases of construction, the first one from 5.3 to 4.0 Ma, and from 3.3 to 1.4 Ma, separated by 700 kyr of erosion or without apparent volcanism. Unfortunately, due to the tropical climate, no soil or discordant contact between the deposits of each stage can be identified to better interpret this hiatus.

Despite some significative differences with published data, we obtained ages on the same order than those published earlier (Westercamp et al., 1989). Few new ages are similar to those obtained earlier from the same outcrop, but with lower uncertainties (Table 1 and 2). The Morne du Lorrain, previously dated at 2.58 ± 0.08 Ma (sample 24; Westercamp et al., 1989), yields a new K-Ar age of 2.55 ± 0.04 Ma on groundmass separates (sample 06MT13, Table 2). Moreover, the quarry "l'Enclos" at Schoelcher was previously dated at 1.87 ± 0.17 Ma (Westercamp et al., 1989) and 1.86 ± 0.03 Ma (Samper et al., 2008), and we obtained an age of 1.86 ± 0.03 Ma for the lava flow of Cascade Absalon (sample 06MT38), which is located several kilometres northward and probably belong to the same eruptive episode or even to the same lava flow. Similar observations can be made in the region of Saint-Pierre where the lava flow along the road D11 yields an age of 1.69 ± 0.02 Ma (Samper et al., 2008), while the cliff of Canal des Esclaves, which belong to the same eruptive stage, yields close ages of 1.75 ± 0.03 (sample 06MT19) and 1.61 ± 0.02 Ma (sample 06MT16), for the base and the top, respectively (Fig. 3).

However, at other locations, some of our ages are quite different with those published. Sample 06MT25 gives an age of 2.12 ± 0.03 Ma for Morne Balisier, which is significatively younger than the earlier age of 2.60 ± 0.10 Ma (Westercamp et al.; 1989). In the same fashion, the massive aphyric lava at Pont de la Campbeilh, was previously dated at 2.60 ± 0.15 Ma (whole-rock K-Ar; Westercamp et al., 1989) and 2.27 ± 0.03 Ma (Samper et al., 2008). We have sampled the same outcrop and obtained a new age of 2.27 ± 0.03 Ma (06MT08) which reinforces the data obtained by Samper et al (2008) and further supports the reproducibility of the full process of the Cassignol-Gillot technique. We note, however, that sample 19, located in the Rivière de Case Pilote and dated at 2.25 ± 0.15 Ma (Westercamp et al., 1989), probably belongs to the same volcanic unit characterized by aphyric basaltic lavas.

5.1.2. Chemical evolution

To better constrain the evolution of Morne Jacob volcano, the new K-Ar ages have been used together with the geochemical data in a diagram showing major and trace elements as a function of the age (Fig. 5). Samples of the first stage have SiO_2 content lower than 55 wt.%, with La/Sm ratio increasing through time, due to magmatic differentiation. During the second stage (from 3.3 to 1.4 Ma), a marked change occurs between 2.27 and 2.12 Ma. First, we observe an increase of SiO_2 content between 3.00 Ma and 2.27 Ma (from 56.30 to 60.65 wt%), while La/Sm ratio remains almost constant around 3.00 ppm. At 2.12 Ma, the La/Sm ratio is significantly higher than for older samples and then decreases from 3.72 to 2.37 ppm, associated to a lowering of the SiO_2 content from 59.80 to 56.20 wt.%. These results allow us to divide the second stage into two phases, the first one from 3.30 to 2.27 Ma characterized by a magma evolving by fractional crystallization, and the second from 2.12 to 1.50 Ma characterized by the eruption of magmas with increasing basic features.

5.1.3. Creeping of the northeastern sector

The first eruptive sequence of Morne Jacob was submarine and built above a basement made of hyaloclastites from the older Vauclin-Pitault submarine chain (Westercamp et al., 1989). The youngest and more basic lava flows are located around the eruptive centre (Morne Jacob summit) inside a U-shaped structure, open to the northeast and underlined by two main rivers. They were also emitted through fissures along the rims, mostly to the south and the west (Fig. 2 and Fig.6). During the initial building stage of a volcano, primitive magmas erupt, but their mass does not generally affect the stress field of the basement

(Borgia, 1994). Then, as the volcano grows and increases its surface load, it can cause compressive stress and prevent the densest magmas from reaching the surface, while evolved magma erupt or intrude the edifice (Borgia, 1994; Borgia et al., 2000; Davidson et al., 2000; Pinel et al., 2000). The less evolved and densest magmas preferentially erupt through weak zones, as the central conduit, faults or depressions caused by sliding and/or flank collapse (Borgia, 1994; Borgia et al., 2000; Davidson et al., 2000; Pinel et al., 2000; Walter et al., 2003). Basement spreading along a décollement within or at the base of the edifice could induce extension of the summit and the upper flanks (Merle et al., 1996) and favour magma ascent along the created faults. It is now admitted that the growth of a volcanic edifice also induces changes in its substrate, such as spreading or creeping (Borgia, 1994; Borgia et al., 2000; Tibaldi et al., 2006). Long-term creep, deforming large sectors of the volcano, can occur if ductile substrata, such as sediments or hydrothermalised rocks underlie the edifice (Borgia, 1994; Tibaldi et al., 2008).

We propose that, in the case of Morne Jacob volcano, which is built over the Vauclin-Pitault submarine chain mainly composed of hyaloclastites (Westercamp et al., 1989), the load of the volcano over this unstable basement, as well as the presence of faults, could have favoured a slow gravitational slide of the volcano, which could be related to creeping. Such slow mass displacement to the northeast formed a depression at the centre of the edifice (Fig. 6), and could have changed the stress field of the substratum and plumbing system, reducing the load above the magma chamber. Then, this allowed densest magmas to reach the surface more easily, and thus influenced the chemistry of erupted products as observed here (Fig. 5), and therefore could also explained physical changes illustrated by lavas flowing over greater distances. Similar responses to spreading have been observed at Concepción Volcano (Borgia et al., 2003) and at Vesuvius (Borgia et al., 2005), among others, where spreading was accompanied and followed by voluminous fissure eruptions with a decrease in VEI and silica

contents. At Morne Jacob shield volcano, we observe a decrease of the time-average eruptive rate of about one order of magnitude, from 0.066 to 0.007 km^3/kyr between the two stages separated by the initiation of the northeast creeping event (Fig. 6). Finally, note that the lack of major flank collapse event related to this slide can be explained by the relatively smooth slope of the Atlantic coast with regard to the Caribbean coast. Effectively, most flank collapses identified in the Lesser Antilles are directed to the west (Deplus et al., 2001; Boudon et al., 2007).

5.2. Carbet complex

Previous studies showed that the older Carbet Complex was active between 2 and 1.8 Ma (Westercamp et al., 1989), based on samples from a pyroclastic flow and a debris flow, respectively. More recently, Samper et al. (2008) showed that the flank collapse (Boudon et al., 2007) occurred between 1.86 ± 0.03 Ma and 341 ± 5 ka, and that the homogeneity of their K-Ar ages on the Pitons du Carbet s.s. is a strong argument for their rapid emplacement (within a few thousand years), subsequently to the collapse.

The older Carbet Complex is built over the western flank of the Morne Jacob volcano. In this area, the basement is composed of lava flows from the last building stage of Morne Jacob erupted between 2.12 and 1.5 Ma. The K-Ar age of 770 ± 10 ka recently obtained on Piton Gelé (Samper et al., 2008) and our new K-Ar ages on Morne Césaire (sample 06MT36, 998 ± 14 ka), Morne Fumé (sample 06MT21, 893 ± 13 ka) and Morne Saint Gilles (sample 07MT123, 603 ± 11 ka), show that the Old Carbet Complex has been constructed more recently than previously inferred, during at least 400 kyr, between 998 ± 14 ka and 603 ± 11 ka. We thus provide an older boundary for the flank collapse event now constrained between 603 ± 11 and 341 ± 5 ka. Our new K-Ar age of 332 ± 9 ka obtained on Piton Boucher

(07MT121, Table 2), one of the Pitons du Carbet s.s. is in fully agreement with the mean age of 337 ± 3 ka calculated by Samper et al. (2008), which further reinforces their collapse age and its occurrence during the oxygen isotopic stage 10 to 9 transition (Quidelleur et al., 2008). Thus, the slightly younger age of 322 ± 9 ka (06MT37, Table 2), obtained for a peripheral flow (Fig. 3) can be related to a later stage. The time-average eruptive rates estimated increased of about one order of magnitude from the first to the second stage (0.012 to 0.5 km^3/kyr). Indeed, the Pitons du Carbet s.s. erupted immediately after the flank-collapse event, which has been interpreted as a period of intensive magma production due to mass deloading.

5.3. Conil Complex

We have dated Morne du Céron at 346 ± 6 ka (06MT18) and Morne à Lianes at 207 ± 3 ka (06MT48) whereas these lava flows were previously dated at 0.64 ± 0.10 Ma (Nagle et al., 1976) and 0.51 ± 0.05 Ma (Westercamp et al., 1989), respectively. Our new K-Ar ages allow us to reconsider the construction of Conil Complex during a 365 kyr interval, between 551 and 186 ka.

Figure 3 shows that the youngest lavas are located in a central inland position with respect to other dated lavas. The morphology of the volcano, assimilated to a cone, let us to propose that the main edifice built between 551 and 304 ka, and that several lava domes and flows erupted through a fissure located on the northern flank between 210 and 186 ka. With an history of 350 kyr and an aerial volume of 44 km^3, we have calculated an eruptive rate of 0.2 km^3 / kyr for the Mount Conil Complex.

5.4. Reconstruction of northern Martinique Island

After 20 Myr of volcanism within southern and south-western Martinique Island (Germa et al., 2008), volcanic activity jumped to the north. Basaltic to basaltic-andesite lava flows of the first stage of Morne Jacob were emitted during 1.5 Myr over the hyaloclastitic basement of the Vauclin-Pitault submarine chain (Fig. 7a) to built a 100 km^3 shield volcano from 5.5 to 4.0 Ma, with an eruptive rate of about 0.066 km^3/kyr. After 700 kyr of quiescence, activity resumed and andesites were emitted during 1.1 Ma over the first shield. There, the accumulation of thick lava flows over an unstable basement and the activation of NW-SE and NE-SW faults may have induced a gravitational slide of the north-eastern sector of the volcano to the north. This creeping induced a slow mass displacement, created a loss of load at the centre of the shield, and favoured erosion to occur along the rims of the structure. Then, from 2.12 Ma, more basic magmas were able to reach the surface, as their ascent was favoured by the presence of faults and the deloading over the plumbing system. From 2.12 to 1.50 Ma, more and more basic magmas were continuously emitted inside and outside the structure, with a thickness averaging 40 m, at a rate of 0.007 km^3/kyr, to built the actual Morne Jacob summit, and reaching the Caribbean coasts (Fig. 7a).

In agreement with the westward migration that affected the whole archipelago as well as southern Martinique, volcanism resumed 500 kyr later on the western flank of the Morne Jacob volcano. There, dacitic and viscous magmas erupted as lava domes and thick lava flows to the south from 1 Ma to 600 ka, along the western rims of the depression previously formed by the sliding of Morne Jacob (Fig. 7). At the same time, between 540 and 350 ka, the northern compartment started to edificate with the building of the Mount Conil (Fig. 7b). At about 340 ka, a flank collapse affected the western flank of the Carbet complex and was immediately followed by the emplacement of 5 km^3 viscous lava domes at about 335 ka

(Samper et al., 2008), associated with pyroclastic flow deposits and a few lava flows, hiding the southern rim of the depression (Fig. 7b). Then, the activity remained concentrated in the area of the Conil complex. Around 210 ka, lava domes and flows erupted from an E-W fissure on the northern flank of Mount Conil, and sommital activity migrated progressively to the south-east (Fig. 7). Then, several lava domes emplaced at the summit and on the southern flank of the cone, and volcanism became more explosive. Activity has been characterized by alternation of St Vincent-, Péléan- and Plinian-type eruptions, and the occurrence of three flank collapse events with emplacement of a new cone inside each horseshoe-shaped structure (LeFriant et al., 2003).

6. Conclusions

A dataset of thirty-one new K-Ar ages has been obtained on lava flows and domes in northern Martinique Island. These data, together with geomorphological and geochemical investigations have helped us to better constrain the successive stages of volcanic building, and allow us to propose the following chronology.

Morne Jacob Volcano is the locus of the first volcanic event of the Recent Arc in Martinique Island, from 5.14 ± 0.07 Ma. After 2 Myr of building, a creeping of the northern flank of the shield initiated and has been followed by the eruption of more basic magma inside a U-shaped depression and above the western flank until 1.53 ± 0.03 Ma. A total erupted volume of 114 km^3 is estimated for the entire volcano before any erosional or creeping processes, with a time-average eruptive rate of 0.032 km^3/kyr. Accordingly to the western migration of the volcanic front across the entire arc, a new edifice, the Carbet Complex has been built above the western flank of Morne Jacob between 998 ± 14 ka and 603

± 11 ka. Around 346 ka, a flank collapse destroyed the western flank of the volcano, and has been immediately followed by the eruption of voluminous lava domes (~ 2 - 10 km^3) between 341 ± 5 and 322 ± 7 ka. Thirty-five kilometres northward, the 44 km^3 of Mont Conil have been built between 534 ± 8 and 189 ± 3 ka, and the volcanic activity migrated 4 km southward to the actual eruptive centre of Montagne Pelée. More precise geomorphologic investigations are in progress to estimate the volumes involved in the flank collapse and erosional processes, which have a great influence on the magma chamber properties and onto the eruption behaviour.

Aknowledgements

This work was supported by ANR Antilles CNRS-INSU. The help of Sylvain Charbonnier during fieldwork was gratefully appreciated. This is LGMT contribution n° XXX.

References

Andreieff, P., Baubron, J.C. and Westercamp, D., 1988. Histoire géologique de la Martinique (Petites Antilles): biostratigraphie (foraminifères), radiochronologie (potassium-argon), évolution volcano-structurale. Géologie de la France, 2-3: 39-70.

Andreieff, P., Bellon, H. and Westercamp, D., 1976. Chronométrie et stratigraphie comparée des édifices volcaniques et formations sédimentaires de la martinique (Antilles Françaises). Bulletin du BRGM (deuxième série), Section IV(n° 4): 335-346.

Bellon, H., Pelletier, B. and Westercamp, D., 1974. Données géochronométriques relatives au volcanisme martiniquais. Comptes Rendus de l'Académie des Sciences (CRAS) de Paris, 279(série D): 457-460.

Blanc, F., 1983. Corrélations chronologiques et géochimiques des formations volcaniques du sud de la Basse-Terre de Guadeloupe (Petites Antilles). Début du cycle récent., Univ. Sci. Medic., Grenoble, 171 pp.

Borgia, A., 1994. Dynamic basis of volcanic spreading. Journal of Geophysical Research, 99(B9): 17791-17804.

Borgia, A., Delaney, P.T. and Denlinger, R.P., 2000. Spreading Volcanoes. Annu. Rev. Earth Planet. Sci., 28: 539-570.

Borgia, A., Tizzani, P., Solaro, G., Manzo, M., Casu, F., Luongo, G., Pepe, A., Berardino, P., Fornaro, G., Sansosti, E., Ricciardi, G.P., Fusi, N., Di Donna, G. and Lanari, R., 2005. Volcanic spreading of Vesuvius, a new paradigm for interpreting its volcanic activity. Geophysical Research Letters, 32(3), 4p.

Borgia, A. and Van Wyk de Vries, B., 2003. The volcano-tectonic evolution of Concepcion, Nicaragua. Bull. Volcanol, 65: 248-266.

Boudon, G., Le Friant, A., Komorowski, J.-C., Deplus, C. and Semet, M.P., 2007. Volcano flank instability in the Lesser Antilles Arc: diversity of scale, processes, and temporal recurrence. Journal of Geophysical Research, 112(B8): 28p.

Boudon, G., Le Friant, A., Villemant, B. and Viode, J.-P., 2005. Martinique. *In:* Lindsay, J.M., Robertson, R.E.A., Shepherd, J.B. & Ali, S.(eds) 2005. *Volcanic Hazard Atlas of The Lesser Antilles* Seismic Research Unit, The University of the West Indies, Trinidad and Tobago, W.I. 127 - 146.

Bouysse, P. and Martin, P., 1979. Caractères morphostructuraux et évolution géodynamique d el'arc insulaire des Petites Antilles (Campagne ARCANTE 1). Bulletin du BRGM, section IV(3/4): 185-210.

Briden, J.C., Rex, D.C., Faller, A.M. and Tomblin, J.-F., 1979. K-Ar geochronology and palaeomagneism of volcanic rocks in the Lesser Antilles island arc. Philosophical Transactions of the Royal Society of London. Series A, Mathematical and Physical Sciences, 291: 485-528.

Carlut, J., Quidelleur, X., Courtillo, V. and Boudon, G., 2000. Paleomagneic directions and K/ar dating of 0-1 Ma lava flows from La Guadeloupe Island (French West Indies): Implications for time averaged field models. Journal of Geophysical Research, 105(B1): 835-849.

Cassignol, C. and Gillot, P.-Y., 1982. Range and effectiveness of unspiked potassium-argon dating: experimental groundwork and applications. In: G.S. Odin (Editor), Numerical dating in Stratigraphy. John Wiley & sons, pp. 159-179.

Davidson, J. and de Silva, S., 2000. Composite Volcanoes. In: Sigurdsson (Editor), Encyclopedia Of Volcanoes. Academic Press, pp. 663-681.

Deino, A. and Potts, R., 1992. Age-probability spectra for examination of single-crystal 40Ar/39Ar dating results: example from Olorgesailie, southern Kenya Rift. Quaternary International, 13/14: 47-53.

Deplus, C., Le Friant, A., Boudon, G., Komorowski, J.-C., Villemant, B., Harford, C., Ségoufin, J., and Cheminée, J.-L., 2001. Submarine evidence for large scale debris avalanches in the Lesser Antilles Arc. Earth and Planetary Science Letters, 192: 145-157.

Fink, L.K., 1972. Bathymetric and geologic studies of the Guadeloupe region, Lesser Antilles island arc. Marine Geology, 12: 267-288.

Frey, H.M., Lange, R.A., Hall, C.M. and Delgado-Granados, H., 2004. Magma eruption rates constrained by 40Ar/39Ar chronology and GIS for the Ceboruco-San Pedro volcanic field, western Mexico. GSA Bulletin, 116(3/4): 259-276.

Germa, A., Quidelleur, X., Labanieh, S. and Chauvel, C., 2008. First radiometric (K-Ar) ages of the oldest volcanism of Martinique Island: Insights about the onset of arc volcanism in the Lesser Antilles, and calibration of the Oligocene / Miocene boundary. International Journal of Earth Sciences, to be submitted.

Gillot, P.-Y. and Cornette, Y., 1986. The Cassignol technique for potassium-argon dating, precision and accuracy: examples from the late pleistocene to recent volcanism from southern Italy. Chemical Geology, 59: 205-222.

Gillot, P.-Y., Hildenbrand, A, Lefèvre J.-C., and Albore-Livadie, C., 2006. The K/Ar dating method: principle, analytical techniques and application ti Holocene volcanic eruptions in southern Italy. Acta Vulcanologica, 18(2): 55-66.

Gillot, P.-Y., Cornette, Y., Max, N. and Floris, B., 1992. Two reference materials, trachytes MDO-G and and ISH-G, for argon dating (K-Ar and 40Ar/39Ar) of Pleistocene and holocene rocks. Geostandards Newsletter, 16(1): 55-60.

Grunevald, H., 1965. Géologie de la Martinique, Mémoires pour servir à l'explication de la carte géologique détaillée de la France, Paris, pp. 144.

Harford, C., Pringle, M., Sparks, R.S.J. and Young, S.R., 2002. The volcanic evolution of Montserrat using 40Ar/39Ar geochronology. *In*: T.H. Druitt and B.P. Kokelaar (Editors), *The Eruption of Soufrière Hills Volcano, Montserrat, from 1995 to 1999*. Geological Society, London, Memoirs. 21: 93-113.

Hildreth, W., Fierstein, J. and Lanphere, M., 2003a. Eruptive history and geochronology of the Mount Baker volcanic field, Washington. Geological Society of America Bulletin, 115(6): 729-764.

Hildreth, W. and Lanphere, M.A., 1994. Potassium-Argon Geochronology of a Basalt-Andesite-Dacite Arc System - the Mount Adams Volcanic Field, Cascade Range of Southern Washington. Geological Society of America Bulletin, 106(11): 1413-1429.

Hildreth, W., Lanphere, M.A. and Fierstein, J., 2003b. Geochronology and eruptive history of the Katmai volcanic cluster, Alaska Peninsula. Earth and Planetary Science Letters, 214(1-2): 93-114.

Hora, J.M., Singer, B. and Wörner, G., 2007. Volcano evolution and eruptive flux on th ethick crust of the Andean Central Volcanic Zone: 40Ar/39Ar constraints from Volcan Parinacota, Chile. GSA Bulletin, 119(3/4): 343-362.

Jicha, B.R. and Singer, B., 2006. Volcanic history and magmaic evolutoin of Seguam Island arc, Alaska. GSA Bulletin, 118(7/8): 805-822.

Labanieh, S., Chauvel, C., Germa, A. and Quidelleur, X., 2008. Two isotopic mixing lines in Martinique Island: The effect of ridge subduction. Geochimica et Cosmochimica Acta, 72(12): A509-A509.

Le Friant, A., Boudon, G., Deplus, C. and Villement, B., 2003. Large-scale flank collapse events during the activity of Montagne Pelée, MArtinique, Lesser Antilles. Journal of Geophysical Research, 108(B1): 13.

Lewis-Kenedi, C.B., Lange, R.A., Hall, C.M. and Delgado-Granados, H., 2005. The eruptive history of the Tequila volcanic field, western Mexico: ages, volumes and relative proportions of lava ypes. Bull. Volc., 67: 391-414.

Merle, O. and Borgia, A., 1996. Scaled experiments of volcanic spreading. Journal of Geophysical Research - Solid Earth, 101(B6): 13805-13817.

Nagle, F., Stipp, J.J. and Fisher, D.E., 1976. K-Ar geochronology of the Limestone Caribees and MArtinique, Lesser Antilles, West Indies. Earth and Planetary Science Letters, 29: 401-412.

Odin, G.S., 1982. Interlaboratory standards for dating purposes. In: Odin (Editor), Numerical dating in stratigraphy, pp. 123-150 (630p).

Pinel, V. and Jaupart, C., 2000. The effect of edifice load on magma ascent beneath a volcano. Philosophical Transactions of the Royal Society of London. Series A, Mathematical and Physical Sciences, 358: 1515-1532.

Quidelleur, X., Gillot, P.-Y., Soler, V. and Lefèvre, J.-C., 2001. K/Ar dating extended into the last millenium: application to the youngest effusive episode of the Teide Volcano (Spain). Geophysical Research Letters, 28(16): 3067-3070.

Quidelleur, X., Hildenbrand, A., Samper, A., 2008. Causal link between Quaternary paleoclimatic changes and volcanic islands evolution. Geophysical Research Letters, 35(2).

Samper, A., Quidelleur, X., Boudon, G., Le Friant, A. and Komorowski, J.C., 2008. Radiometric dating of three large volume flank collapses in the Lesser Antilles Arc. Journal of Volcanology and Geothermal Research, 176: 485-492.

Samper, A., Quidelleur, X., Lahitte, P. and Mollex, D., 2007. Timing of effusive volcanism and collapse events within an oceanic arc island: Basse-Terre, Guadeloupe archipelago (Lesser Antilles Arc). Earth and Planetary Science Letters, 258(1-2): 175-191.

Steiger, R.H. and Jäger, E., 1977. Subcommission on Geochronology: convention on the use of decay constants in Geo and Cosmochronology. Earth and Planetary Science Letters, 36(3): 359-362.

Tibaldi, A., Corazzato, C., Kozhurin, A., Lagmay, A.F.M., Pasquarè, F.A., Ponomareva, V.V., Rust, D., Tormey, D. and Vezzoli, L., 2008. Influences of substrate tectonic heritage on the evolution of composite volcanoes: Predicting sites of flank eruption, lateral collapse, and erosion. Global and Planetary Change, 61(3-4): 161-174.

Tibaldi, A. and Lagmay, A.F.M., 2006. Interaction between volcanoes and their basement. Journal of Volcanology and Geothermal Research, 158: 1-5.

Walter, T.R. and Troll, V.R., 2003. Experiments on rift zone evolution in unstable volcanic edifices. Journal of Volcanology and Geothermal Research, 127: 107-120.

Westercamp, D., 1972. Contribution à l'étude du volcanisme en Martinique, Université Paris-Sud, Orsay, 278 pp.

Westercamp, D., Andreieff, P., Bouysse, P., Cottez, S. and Battistini, R., 1989. Martinique; Carte géologique à 1/50 000,. In: BRGM (Editor).

Westercamp, D. and Tazieff, H., 1980. Martinique, Guadeloupe, Saint-Martin, La désirade. Masson, Paris, 135 pp.

Figures Caption

Figure 1 A: Geodynamic setting of the Lesser Antilles Arc. Bathymetry from Smith and Sandwell, 1997.

Figure 1 B: Schematic geological map of Martinique Island, after Westercamp et al., 1989. 1: Basal Complex and Sainte Anne Series, 2: Vauclin-Pitault submarine chain, 3: South-Western Volcanism, 4: Trois Ilets Volcanism, 5: Morne Jacob Shield Volcano, 6: Carbet Complex, 7: Conil Complex, 8: Mount Pelée.

Figure 2: Top: Relief map of northern Martinique Island with the main summits.
Bottom: Digital elevation model and schematic geologic map of northern volcanic units (after Westercamp et al., 1989). Location of the 57 sampling sites. White squares are for Mount Conil dated samples, white circles are for Morne Jacob dated samples, white diamonds are for Carbet Complex dated samples. Blacks symbols are for non dated samples.
Black lines show the three flank-collapse structures that affected Mount Pelée (after Le Friant et al., 2003). White lines are for Carbet Complex flank-collapse (after Boudon et al., 2005).

Figure 3: Northern Martinique Island shaded digital elevation model with the schematic geologic map (after Westercamp et al., 1989).Cassignol-Gillot K-Ar ages are reported within each volcanic complex (same symbols as in Fig.2). Ages are in Ma, otherwise indicated in ka.

Figure 4: Age probability spectra (ideogram) from Deino and Potts (1992) showing the periods of volcanic activity for Morne Jacob shield Volcano.

Figure 5: SiO_2 and La/Sm ratio evolution through time for Morne Jacob samples. Geochemical data from Labanieh et al., 2008.

Figure 6: Digital elevation model viewed from the north-east. Location of the Morne Jacob dated samples from stage 1 (green) and stage 2 (yellow). Ages are in Ma. Dashed white line underlines the creeping structure. The arrow shows the direction of the mass displacement. Schematic representation of volcanic spreading process, modified from Merle and Borgia, 1996.

Figure 7: Evolution of northern Martinique Island through time. 3D views from SW from reconstructed edifices without flank collapse events.a: 5.5 – 4.0 Ma, b: 3.3 – 2.2 Ma, c: 2.2 – 2.1 Ma, d: 2.1 – 1.5 Ma, e: 1 Ma – 600 ka, f: 340 ka, g: 340 – 190 ka, h: 190 ka – present.

Table 1: Published ages for Morne Jacob, Carbet Complex, Conil Complex and Mount Pelée.

Table 2: New K-Ar ages obtained in this study. Column headings indicate sample name, name of the site location, Longitude and latitude, the dated mineral phase, potassium concentration in percent, concentration of radiogenic (*) $_{40}Ar^*$ in percent, number of atoms/g of radiogenic ^{40}Ar, age and 1 sigma uncertainy, weighted mean ages and weighted uncertainty.

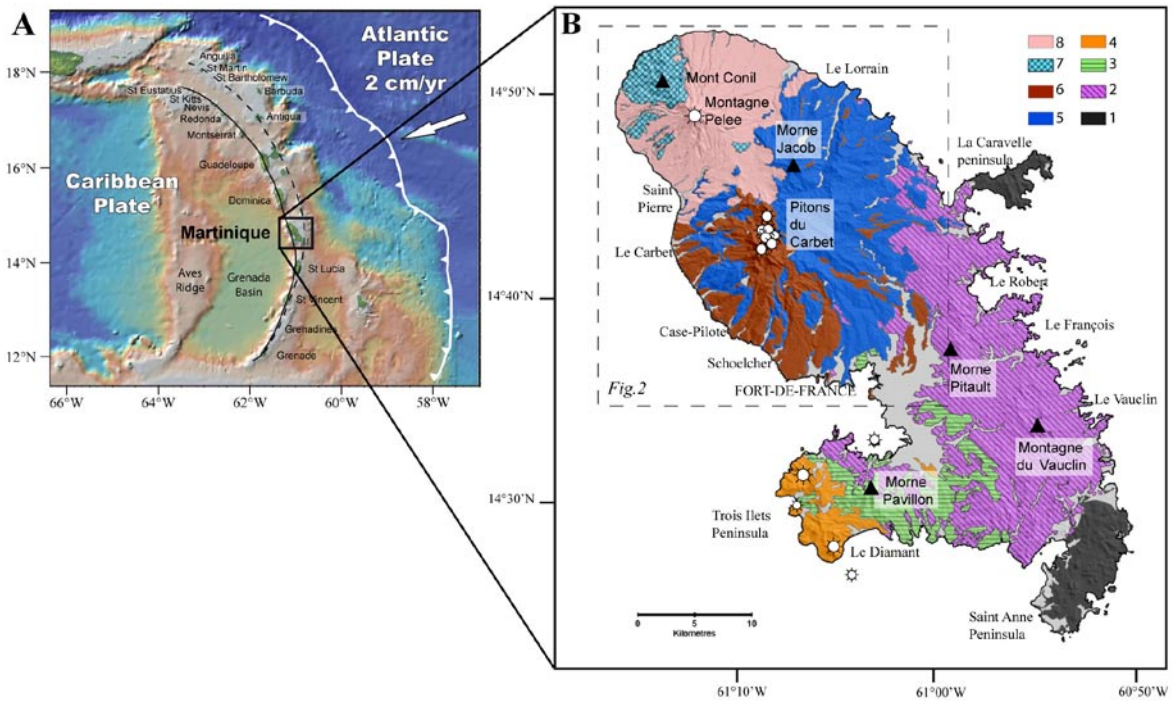

Fig. 1

(Germa et al., 2008)

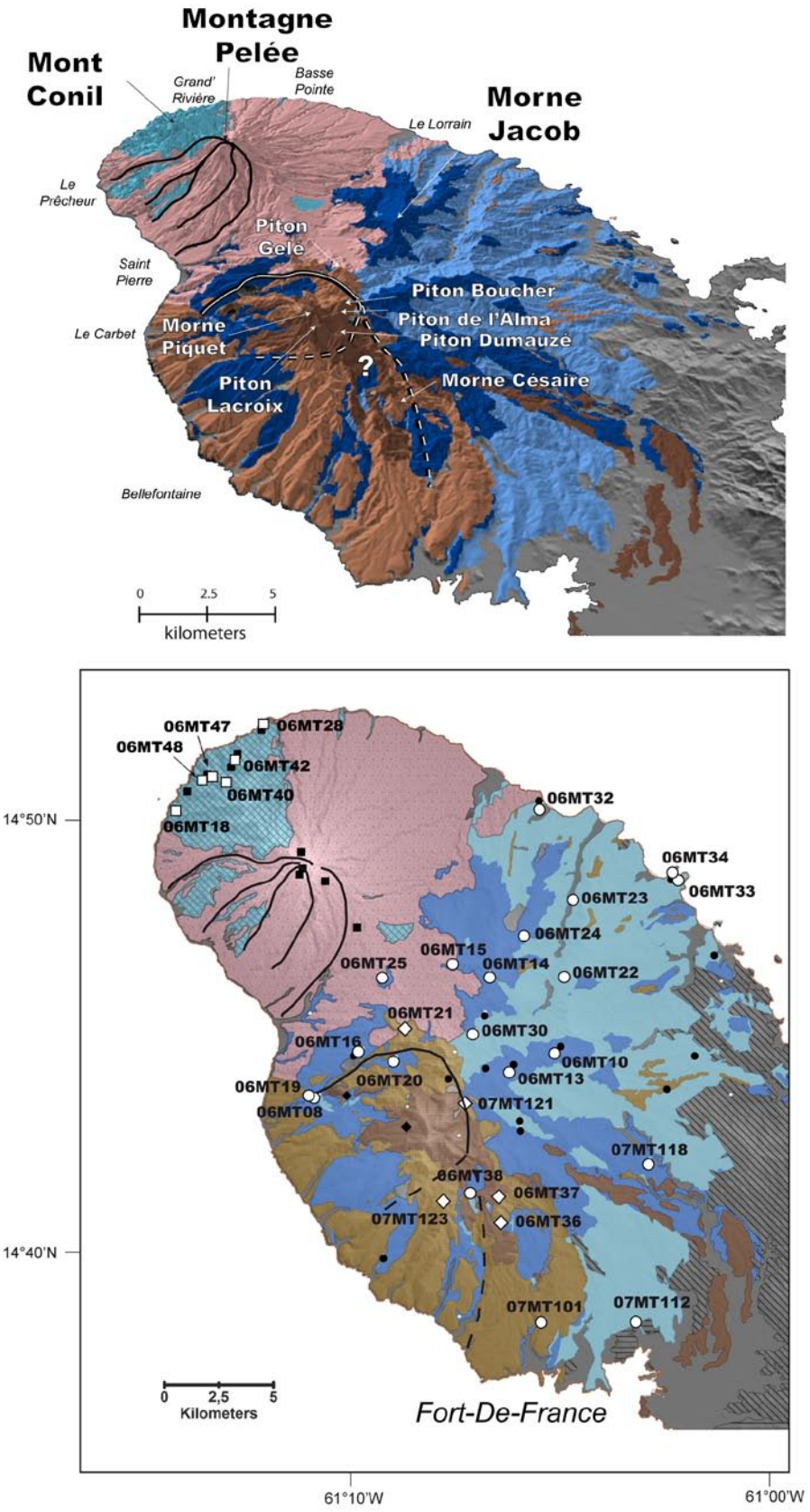

Fig. 2

Germa et al., 2008

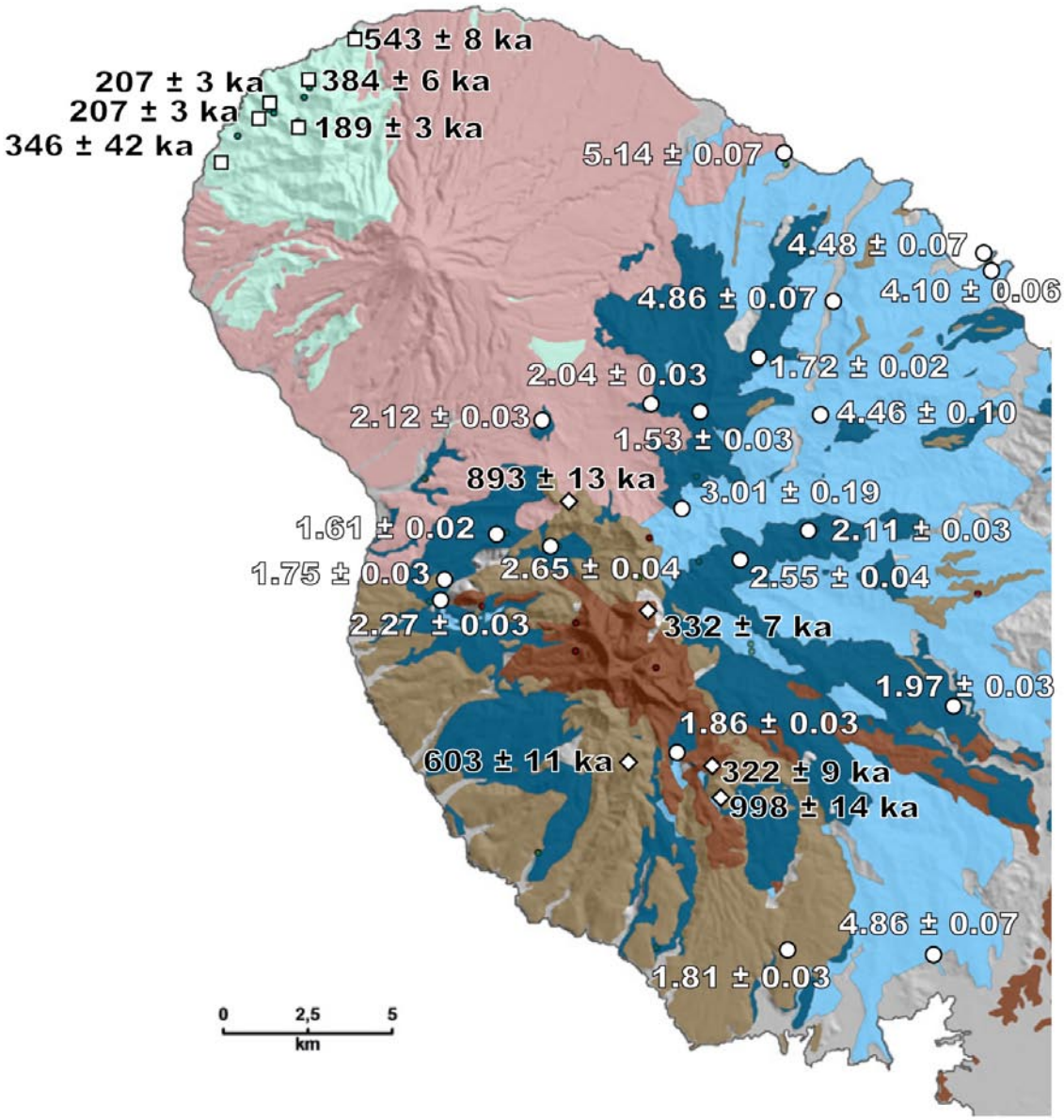

Fig. 3

Germa et al., 2008

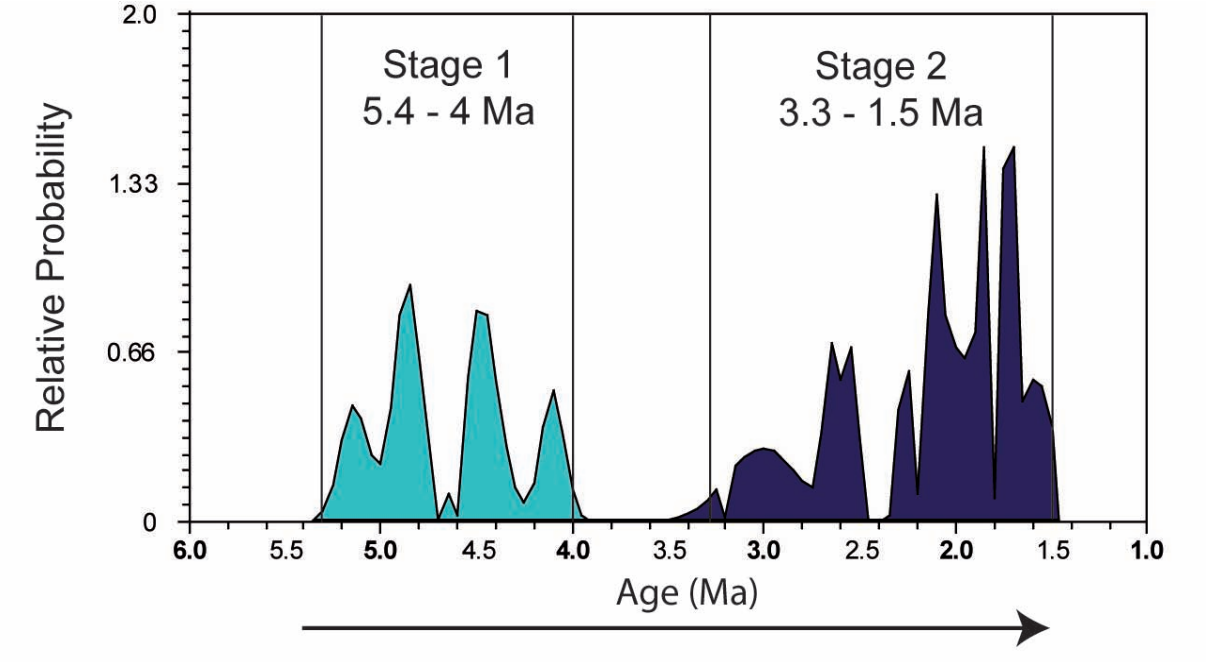

Fig. 4

Germa et al., 2008

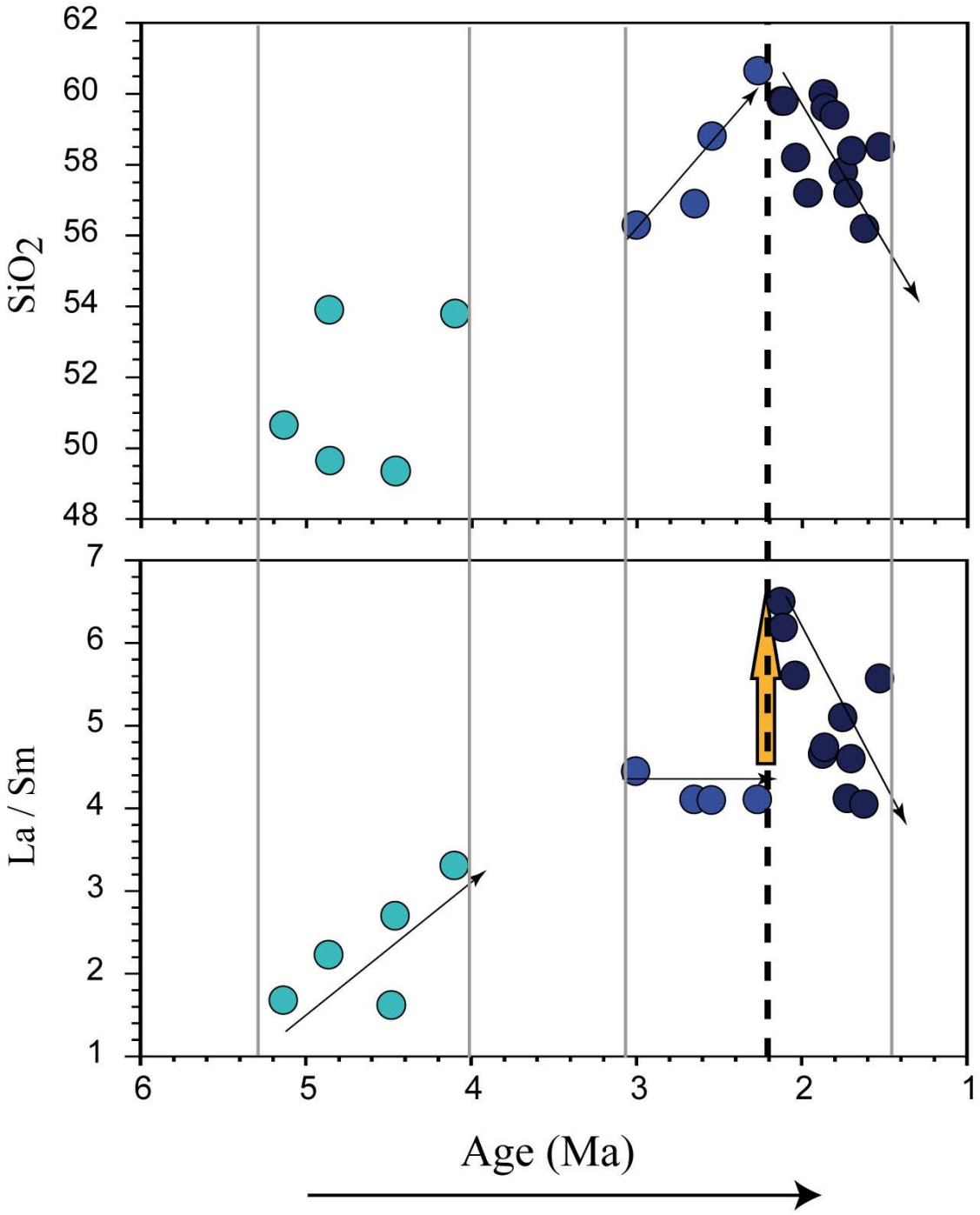

Fig. 5

Germa et al., 2008

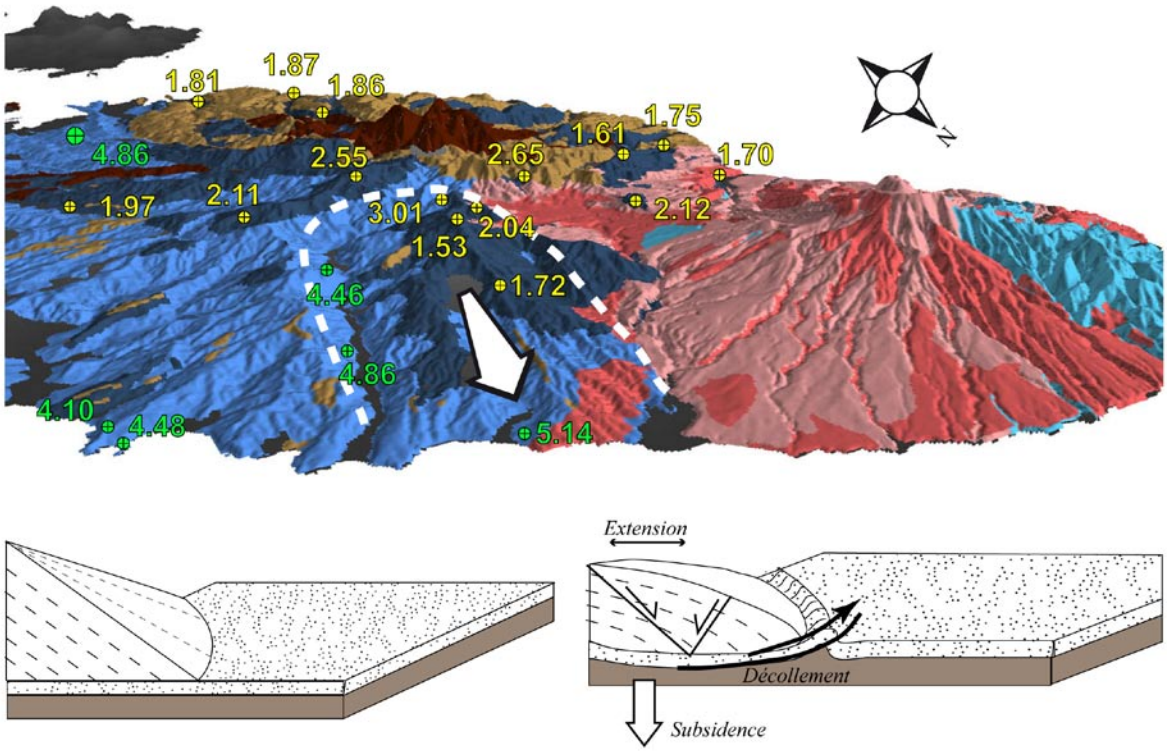

Fig. 6

Germa et al., 2008

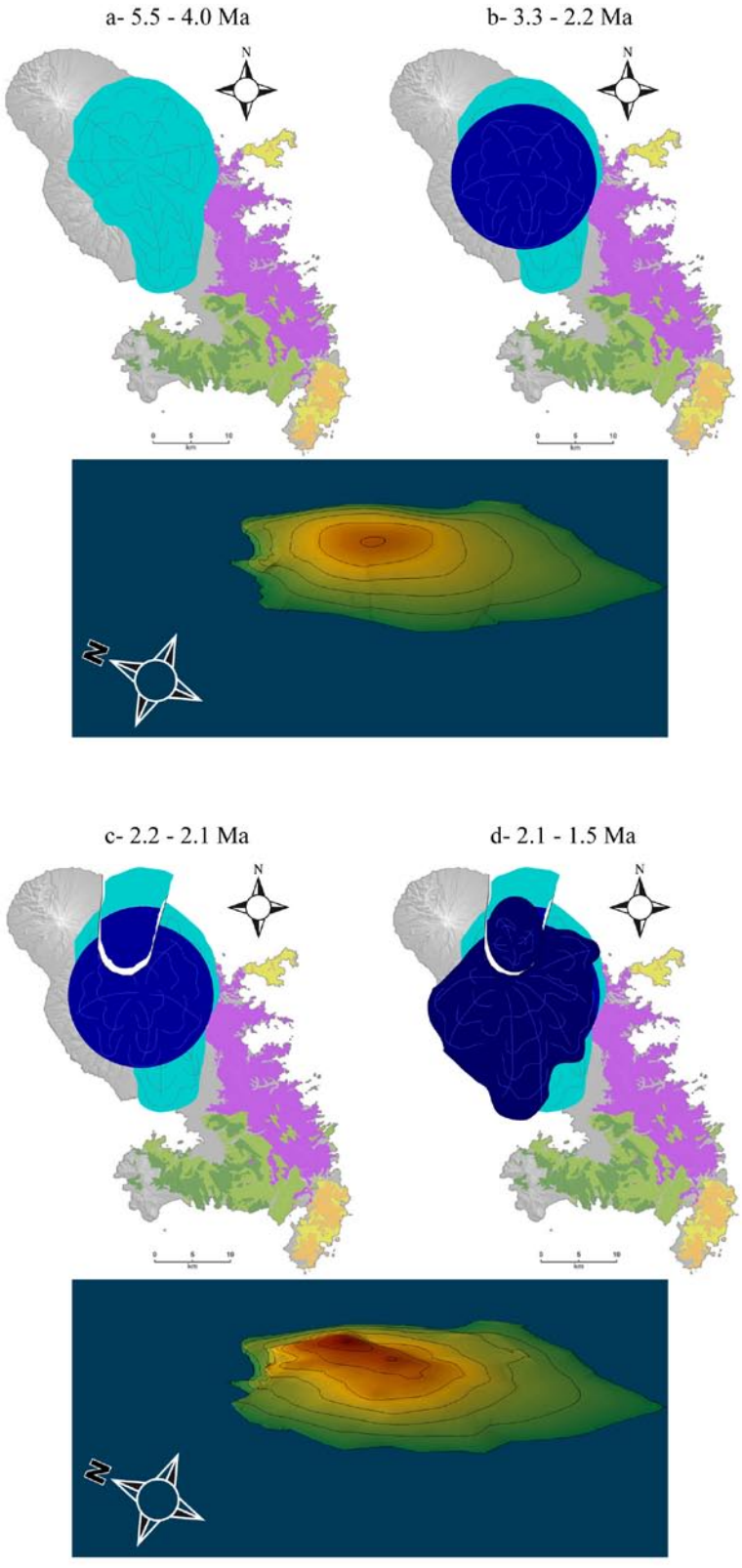

Fig. 7

Germa et al., 2008

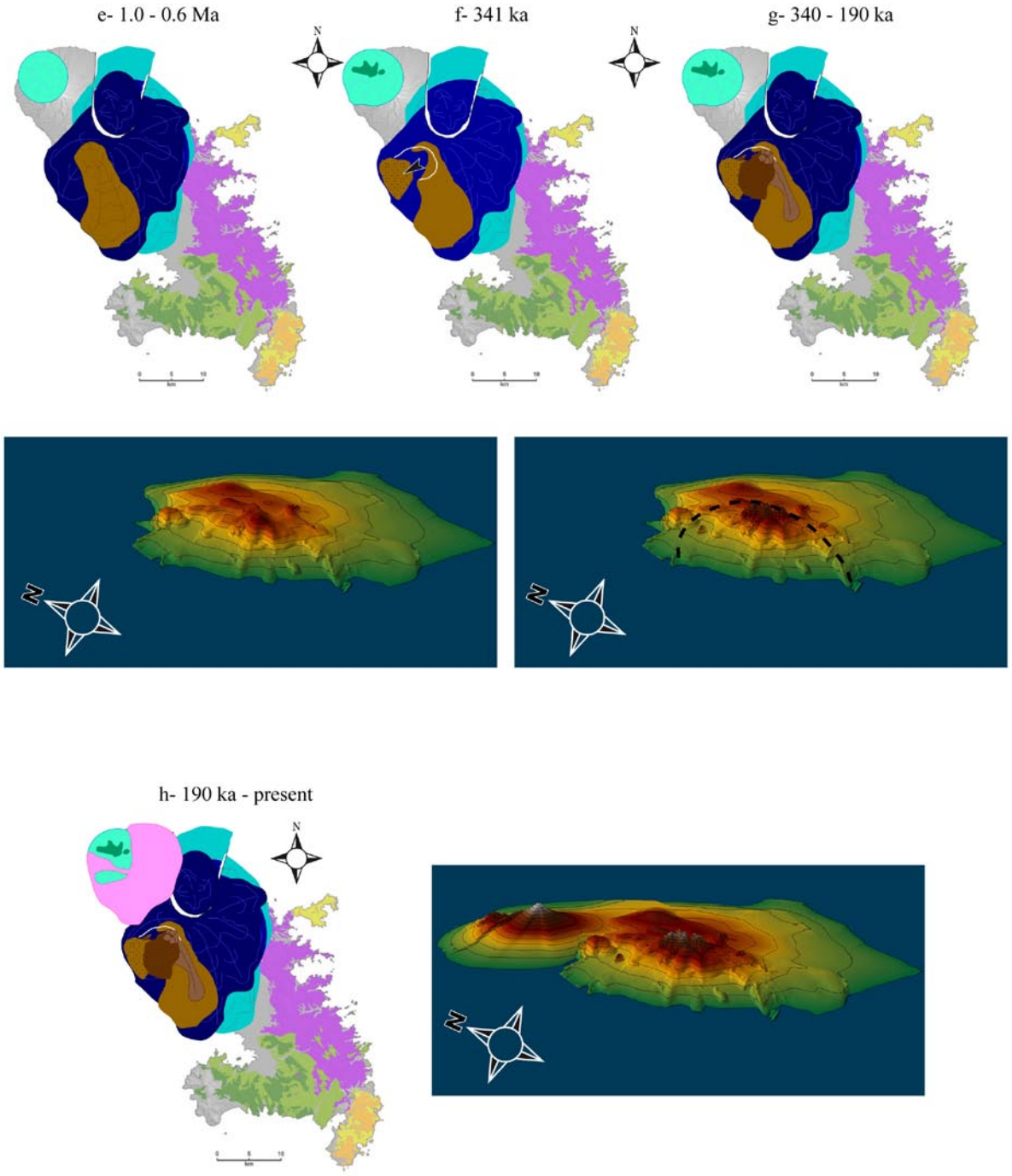

Fig. 7 (continued)

Germa et al., 2008

Sample (ref)	Location	K (%)	Age ± 1sigma (Ma)
	Morne Jacob		
04MT08 (*)	La Plassonerie	1.545	2.27 ± 0.030
04MT04 (*)	L'Enclos	1.680	1.86 ± 0.030
04MT01 (*)	Bellevue – Parnasse	1.523	1.69 ± 0.020
38 (**)	Morne Moco	0.56	4.37 ± 0.25
36 (**)	Pointe Marigot	1.12	4.07 ± 0.20
19 (**)	Case Pilote	1.23	2.25 ± 0.15
26 (**)	Morne Balisier	1.55	2.60 ± 0.10
24 (**)	Morne du Lorrain	1.02	2.58 ± 0.08
	Carbet Complex		
04MT06 (*)	Piton Gelé	1.276	0.770 ± 0.011
7 (**)	Piton Gelé	1.13	1.06 ± 0.10
04MT07 (*)	Piton Man Roy	1.276	0.341 ± 0.005
ALMA (*)	Piton Alma	1.183	0.338 ± 0.005
04MT02 (*)	Morne Piquet	1.271	0.331 ± 0.005
14 (**)	Carrière Schoelcher	1.25	1.87 ± 0.17
18 (**)	Anse madame Marigot	1.10	2.10 ± 0.10
13 (**)	Balata	1.24	1.81 ± 0.15
16 (**)	Balata	1.25	2.02 ± 0.20
5 (**)	Piton Dumauzé	0.77	0.86 ± 0.10
	Conil Complex		
9 (**)	Mont Conil	0.74	1.20 ± 0.20
4 (**)	Morne du Céron	0.72	0.64 ± 0.10
2 (**)	Morne à Lianes	1.02	0.51 ± 0.05
1 (**)	Morne du Bourg	0.94	0.40 ± 0.20
	Montagne Pelée (^{238}U / ^{230}Th)		
(***)	Tombeau des Caraibes	/	0.063 ± 0.010
(***)	Rivière du Precheur	/	0.033 ± 0.005
(***)	Montagne d'Irlande	/	0.039 ± 0.005
(***)	Morne Calebasse	/	0.044 ± 0.005
(***)	Morne Plume	/	0.025 ± 0.003
(***)	Aileron	/	0.010 ± 0.001
(***)	Sans Nom	/	0.009 ± 0.001

Table 1 (Germa et al., 2008)

(*) Samper et al., 2008
(**) Westercamp et al., 1989
(***) Boudon et al., 2005

Sample	Location	Long W	Lat N	Material	K (%)	40Ar* (%)	40Ar*×10^{12} (at/g)	Age ± 1σ (Ma)	Mean age ± 1σ (Ma)
MORNE JACOB VOLCANO									
06MT32	En Bas Bois	61°03.36'	14°50.12'	gms	0.435	27.6	2.339	5.14 ± 0.08	**5.14 ± 0.07**
						29.1	2.336	5.13 ± 0.07	
				plg	*0.017*	*1.8*	*0.084*	*4.89 ± 0.29*	
06MT23	Hab° Durand	61°02.46'	14°48.00'	gms	0.574	18.1	2.898	4.83 ± 0.07	**4.86 ± 0.07**
						33.4	2.931	4.88 ± 0.07	
07MT112	Basse Gondo	61°01.19'	14°37.30'	gms	0.730	24.5	3.703	4.85 ± 0.07	**4.86 ± 0.07**
						20.8	3.716	4.87 ± 0.07	
06MT22	Piton Laroche	61°06.47'	14°26.22'	gms	0.148	5.3	0.683	4.41 ± 0.10	**4.46 ± 0.10**
						5.6	0.697	4.50 ± 0.10	
06MT33	Pointe Pain de Sucre	61°00.17'	14°48.39'	gms	0.396	17.5	1.850	4.47 ± 0.07	**4.48 ± 0.07**
						17.0	1.864	4.50 ± 0.07	
06MT34	Pain de Sucre	61°00.09'	14°48.30'	gms	0.702	28.1	3.017	4.11 ± 0.06	**4.10 ± 0.06**
						20.9	3.001	4.09 ± 0.06	
06MT30	Trace Jésuites	61°04.34'	14°26.21'	gms	0.120	1.8	3.998	3.19 ± 0.18	**3.01 ± 0.19**
						1.4	3.488	2.78 ± 0.20	
06MT20	Fonds Saint Denis	61°07.24'	14°44.06'	gms	1.493	20.9	4.120	2.64 ± 0.04	**2.65 ± 0.04**
						24.1	4.144	2.66 ± 0.04	
06MT13	Morne du Lorrain	61°07.54'	14°26.22'	gms	1.521	14.8	4.019	2.53 ± 0.04	**2.55 ± 0.04**
						26.7	4.062	2.55 ± 0.04	
06MT08	Pont de la Campbeilh	61°09.22'	14°43.11'	gms	1.505	58.0	3.579	2.27 ± 0.03	**2.27 ± 0.03**
06MT25	Morne Balisiser	61°06.14'	14°26.21'	gms	2.005	69.8	4.443	2.12 ± 0.03	**2.12 ± 0.03**
						75.6	4.458	2.13 ± 0.03	
06MT10	Morne Bellevue	60°59.47'	14°44.15'	gms	1.996	80.5	4.343	2.08 ± 0.03	**2.11 ± 0.03**
						78.9	4.467	2.14 ± 0.03	
06MT15	Morne La Piquonne	61°07.21'	14°46.11'	gms	1.604	47.4	3.459	2.06 ± 0.03	**2.04 ± 0.03**
						65.3	3.386	2.02 ± 0.03	
07MT118	St Etienne	61°00.55'	14°41.30'	gms	1.300	45.1	2.689	1.98 ± 0.03	**1.97 ± 0.03**
						54.3	2.769	1.96 ± 0.03	
06MT38	Cascade Absalon	61°02.20'	14°26.20'	gms	1.687	67.8	3.287	1.86 ± 0.03	**1.86 ± 0.03**
						62.9	3.282	1.86 ± 0.03	
07MT101	Ravine Vilaine	61°03.44'	14°37.31'	gms	1.575	39.9	2.954	1.80 ± 0.03	**1.81 ± 0.03**
						54.2	2.987	1.82 ± 0.03	
06MT19	Canal des esclaves	61°09.32'	14°43.13'	gms	1.625	25.9	2.945	1.73 ± 0.03	**1.75 ± 0.03**
						51.4	2.983	1.76 ± 0.03	
06MT24	Morne Quatre-Vingt	61°04.04'	14°47.08'	gms	1.592	45.9	2.878	1.73 ± 0.02	**1.72 ± 0.02**
						43.5	2.850	1.71 ± 0.02	
06MT16	Morne des Cadets	61°08.27'	14°44.19'	gms	1.179	42.6	1.971	1.60 ± 0.02	**1.61 ± 0.02**
						53.9	2.002	1.63 ± 0.02	
06MT14	Morne Jacob	61°04.59'	14°46.11'	gms	1.523	38.3	2.422	1.52 ± 0.02	**1.53 ± 0.03**
				gms	1.544	57.4	2.481	1.54 ± 0.02	
				plg	*0.312*	*14.9*	*0.491*	*1.51* ± 0.02	

Table 2 (Germa et al., 2008)

Sample	Location	Long W	Lat N	Material	K (%)	40Ar* (%)	40Ar*×10^{12} (at/g)	Age ± 1σ (Ma)	Mean age ± 1σ (ka)
CARBET COMPLEX									
06MT36	Morne Césaire	61°03.27'	14°26.20'	gms	2.011	52.5	2.097	998 ± 14	**998 ± 14**
						60.2	2.095	997 ± 14	
				plg	*0.214*	*13.3¨*	*0.329*	*1471 ± 24*	***1492 ± 24***
						13.5	*0.338*	*1513 ± 24*	
06MT21	Morne Fumé	61°07.15'	14°44.49'	gms	1.761	45.0	1.658	901 ± 13	**893 ± 13**
					1.761	49.1	1.629	885 ± 13	
06MT37	Plateau Courbaril	61°02.54'	14°26.20'	gms	0.756	9.9	0.246	311 ± 5	**322 ± 9**
						9.6	0.255	322 ± 6	
						8.6	0.265	335 ± 6	
07MT121	Piton Boucher	61°05.42'	14°42.58'	gms	1.253	18.78	0.423	323 ± 5	**332 ± 7**
						22.72	0.444	340 ± 8	
07MT123	Morne Saint Gilles	61°06.13'	14°40.37'	gms	1.286	20.79	0.809	603 ± 11	**603 ± 11**
CONIL COMPLEX									
06MT28	Grand' Rivière	61°10.42'	14°52.23'	gms	0.897	21.4	0.515	550 ± 8	**543 ± 8**
						23.4	0.503	537 ± 8	
06MT42	Rivière des Ecrevisses	61°00.07'	14°28.18'	gms	0.785	17.3	0.318	388 ± 6	**384 ± 6**
						10.3	0.308	376 ± 6	
06MT18	Morne du Céron	61°12.56'	14°50.16'	gms	0.888	0.9	0.337	364 ± 42	**346 ± 42**
						0.8	0.301	325 ± 43	
06MT48	Morne à Lianes	60°56.47'	14°26.17'	gms	1.491	26.7	0.322	207 ± 3	**207 ± 3**
						27.9	0.322	207 ± 3	
06MT47	Ravin de l'eau	60°57.20'	14°26.17'	gms	1.177	19.8	0.258	210 ± 3	**207 ± 3**
						20.7	0.250	204 ± 3	
06MT40	Rivère Trois Bras	61°01.14'	14°26.19'	gms	1.069	13.2	0.211	189 ± 3	189 ± 3
						11.9	0.211	189 ± 3	

Table 2 (continued)

(Germa et al., 2008)